Journal of Computers Vol. 33 No. 6, December 2022, pp. 37-50
doi: 10.53106/199115992022123306003

Predicting Temperature-induced Deflection and Abnormality Recognition of Cable-stayed Bridge Based on Machine Learning

Shou-Wang Sun[1], Zhi-Wen Wang[1*], You-Liang Ding[2], Zi-Xiang Yue[2]

[1] Shenzhen Express Engineering Consulting Co., Ltd., Shenzhen 518000, China
1474541490@qq.com, terterter1@126.com
[2] Key Laboratory of C&PC Structures of the Ministry of Education, Southeast Univ., Nanjing 210096, China
civilding@hotmail.com, viscarialight@126.com

Received 9 March 2022; Revised 26 June 2022; Accepted 6 July 2022

Abstract. The vertical deflection of the main girder on a cable-stayed bridge is a direct reflection of the vertical stiffness of bridge structure, which represents the comprehensive mechanical performance of cable-stayed bridge. Compared with the deflection caused by vehicles, the deflection caused by temperature is often more significant and the change frequency is very low, which is easy to extract from raw data, and can be used as an index to evaluate the state of cable-stayed bridge. To obtain the control value for recognizing the abnormal deflection, it is necessary to establish an accurate input-output relationship between temperature and temperature-induced deflection. However, because of the high-order nonlinear relationship between the temperature and the temperature-induced deflection, the traditional linear regression is not accurate enough in modeling this relationship. To establish a high-precision model for the deflection, this paper uses the machine learning tools with the highly nonlinear fitting performance to further model the project. Considering both the precision and modeling efficiency, the Long-Short Term Memory (LSTM) network can build the optimal model between temperature and temperature-induced deflection. Use the regression value output by LSTM as the control value combining with the statistical pattern of t-test, the 6% abnormal deflection can be recognized. The 6% sensitivity can help to recognize bridge abnormalities earlier.

Keywords: structural health monitoring, cable-stayed bridge, temperature-induced deflection, machine learning, LSTM model

1 Introduction

Transportation plays a fundamental role in the daily life. As the key in transportation, bridges play the role of lifeline and are the indispensable part of infrastructure construction.

The bridge health monitoring system is a method combining bridge structure theory, test sensing technology and other multidisciplinary fields. Its basic connotation is to monitor and evaluate the health status of bridge structure by collecting various data during bridge operation, to provide basis and guidance for bridge maintenance [1]. With the help of health monitoring systems, the real-time temperature field amd displacement response can be studied and analyzed, to grasp the actual structural performance of the bridge and ensure the safety of bridge.

The research of the temperature field based on the health monitoring data is an important topic. The temperature displacement of bridge is no le ss than the internal force caused by dead weight and live load [2]. It can be seen that temperature is one of the important factors affecting the service life of bridge structure.

The bridge damages will cause serious losses. American scholars observed the bearing reaction of a champigny box girder bridge, and they found that the temperature difference caused about 26% variation of bearing reaction. In China, the cracks have been found in Jiujiang Yangtze River Bridge and Xicheng bridge, and these cracks are closely related to temperature. It can be seen that the temperature has an important impact on the bridge structure. Relying on the health monitoring data, it is important to establish the prediction modelto find and control the temperature responseand ensure the bridge safety.

Since the 1960s, researchers in various countries have done a lot of work on the spatial distribution, influencing factors and prediction methods of the temperature response. Some scholars use mathematical theory to analyze the collected meteorological data, to deduce the factors that affect the temperature distribution of the girder of a bridge, and put forward the linear distribution of temperature effect [3]. In New Zealand, some scholars have carried out several model tests on one viaduct, and proposed the formulas to predict the temperature distribution along the concrete box girder [4-5]. Hoffman obtained the factors influencing the nonlinear temperature distribu-

* Corresponding Author

tion of a prestressed concrete box girder through the long-term observation of bridge temperature [6]. With the development of finite element theory and computer technology, temperature field can be analyzed and summarized by finite element method [7]. In China, a thin-walled hollow high pier is modeled by finite element to fit its temperature difference curve [8-10]. Based on the measured temperature of Hongshuihe cable-stayed bridge and Jiujiang Yangtze River Bridge, Liu Xing analysed the temperature stress of a prestressed concrete box girder [8-10]. Temperature gradient model of one cross-sea bridge has been analysed by both finite element method and entity model. [11-12]. Based on the monitoring data of Runyang Bridge, the whole life simulation method of the temperature field of a flat steel box girder is put forward [13].

To sum up, scholars have done a lot of work on the temperature field and the prediction of the temperature field, including the actual test, theoretical formulas, finite element simulation and many other aspects.

In the past decades, relying on the rapid developing infrastructure, many major bridges have been installed with health monitoring systems. Massive temperature data and response data from the monitoring system have been obtained. However, the computational cost of these theories or finite element methods is too high, leading to inconvenience for application. Because the data-driven model is not only convenient to apply but also can accurately express the actual state of the service bridge, further research is needed to explore the value of monitoring data and data driven model.

The change of the vertical deflection of the cable-stayed bridge is usually caused by traffic and temperature load, and the change of vertical deflection caused by temperature is often more significant. Therefore, the temperature induced deflection is an important representation of the mechanical performance of cable-stayed bridge. If the regression model with high accuracy can be established between temperature and temperature induced deflection, it not only means that the accurate extraction of temperature induced deflection, but also means that the control value of the deflection of the bridge on is obtained.

For cable-stayed bridges, it is difficult to accurately establish the temperature induced deflection of cable-stayed bridge by conventional regression methods because of the nonlinearity in the relationship between the temperature and the deflection. Therefore, new technologies are needed to solve this highly nonlinear problem.

The birth of machine learning provides an excellent tool for fitting model with nonlinear problems. Using machine learning technology or more advanced means is possible to solve the modeling of temperature induced deflection of cable-stayed bridge. Compared with traditional machine learning tools, such as BPNN (back propagation neural network) [14] or SVM (support vector machine) [15], deep neural network has the ability to express more complex relationships. LSTM (long and short term memory) has the ability to express time series nonlinearity, which is very suitable with the requirements of modeling the deflection introduced by temperature.

Machine learning algorithms are still less used for the deflection model of cable-stayed bridge. So it is important to know if the traditional SVM and BPNN are enough for establishing the model, or the advanced LSTM and more advanced tools should be used. So we must conduct a comparative study of these tools, to analyze the computational cost and accuracy of the calculation results of the different methods. Thus, the best modeling tool is sought in different methods. Finally, we use the best selected tool and the combined statistical test to explore the minimum anomalous deflection that can be detected.

2 Data from Monitoring System

The temperature and deflection data of this paper come from a bridge in the middle reaches of the Yangtze River. Fig. 1 shows the information of the bridge and the monitoring system. As shown in Fig. 1(a), the main girder is the continuous steel truss and the two towers are H-shaped concrete structure. The total length of this bridge is 1218.5 m. For the main span, the length is 567 m.

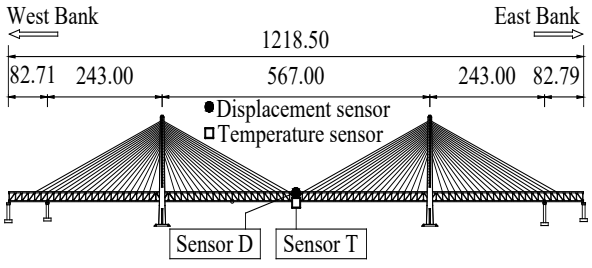

(a) Elevation of the bridge

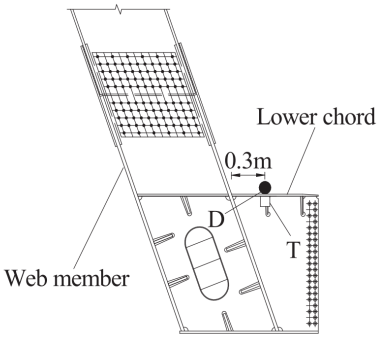

(b) Front view of the location of the sensors in the main girder

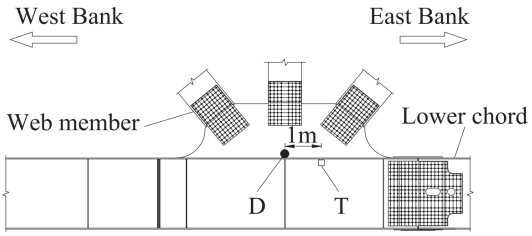

(c) Side view of the location of the sensors in the main girder

Fig. 1. Bridge and bridge monitoring system

Fig. 1(b) and Fig. 1(c) shows the detailed locations of sensors installed on the main girder. The bridge connects the West Bank and the East Bank of the Yangtze River. A vertical displacement sensor, named D, is installed in the middle of the main span. Steel structure temperature sensor, named T, is also installed in the middle of the main span. The sampling frequency of the two sensors is 1Hz. As shown in Fig. 2, in the displacement data of sensor D, a lot of high-frequency information can be seen in the original data. These high-frequency signals, which are the deflection caused by the vehicle, looks like a lot of spikes. To model the temperature-induced deflection, it is necessary to extract the temperature-induced deflection. The temperature-induced deflection can be extracted by being averaged every given time period. Most of the existing studies use the hourly or daily averaging method to extract the temperature induced deflection [16-17]. Although the extracted data is smooth and reflects the characteristics of the temperature-induced deflection, it leads to the decline of real-time performance. To ensure the appropriate data scale and timeliness, this paper uses the ten minute averaging method to extract the temperature-induced deflection. As shown in Fig. 2, the ever ten minute averaged data also maintains a considerable degree of smoothness, so this paper takes the ever ten minute averaged deflection data as the extracted temperature-induced deflection.

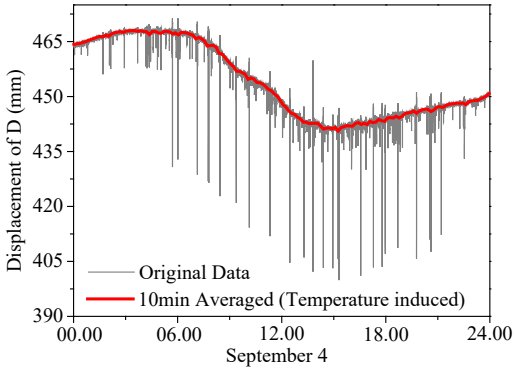

Fig. 2. Original deflection data and temperature-induced deflection

The deflection data of sensor D after being averaged every ten minutes is named as *D*, and the temperature data of sensor T is named as *T* after being averaged every. With the time interval of 10 min, one day has 144 data points.

The time history curves of temperature and deflection are shown in Fig. 3. In this paper, the data during 11 months are used for data mining. Compared with many existing studies, the amount of data in this paper is much larger, to ensure that the research results have higher reliability. After removing the vacancy value, there are 45,648 data points remain in temperature and deflection respectively.

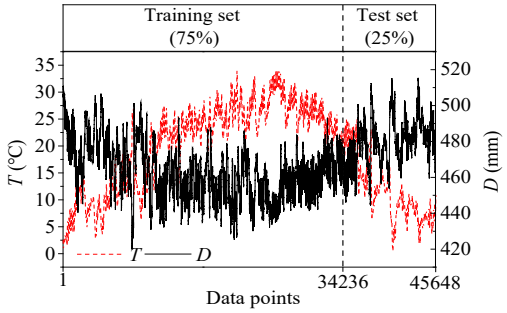

Fig. 3. Time history curves of temperature and deflection

Based on these data, we will use different kinds of fitting tools to establish the relationship between T and D, that is, modeling the temperature-induced deflection.

In addition to use the common linear regression to establish the correlation model between T and D, this paper will also use machine learning algorithms to establish the input-output model based on the similar mode of the time series modeling. We first introduce the machine learning algorithms.

3 Traditional Machine Learning Algorithm

3.1 Support Vector Machine (SVM)

Support vector machine (SVM) is a machine learning algorithm based on statistical learning theory. It has strong high-order expression performance. So SVM is often used for nonlinear regression analysis [18]. In SVM, nonlinear mapping function φ(x) is usually used for mapping x to high-dimensional vector, so the high-order correlation between the input sample x and the predicted value y can be expressed. The regression value is y' can be expressed as follow:

$$y' = \omega \cdot \varphi(x) + b, \tag{1}$$

where ω is weight coefficient, b is bias.

Use the insensitive damage function, ε, to expresses the model error. Then the calculation formula of the training error is as follow:

$$|y - y'|_{\varepsilon} = \begin{cases} 0 & |y - y'| \le \varepsilon \\ |y - y'| - \varepsilon & |y - y'| > \varepsilon \end{cases}. \tag{2}$$

Equal the regression analysis as objective optimization analysis. The relaxation factors, ζ_i and ζ_i*, are introduced into SVM algorithm, and the objective function and constraints can be constructed as Eq.(3) and Eq.(4):

$$\min \frac{1}{2}\|\omega\|^2 + C\sum_{i=1}^{n}(\zeta_i + \zeta_i^*) , \tag{3}$$

$$\begin{cases} y_i - \omega \cdot x_i - b \le \varepsilon + \zeta_i \\ \omega \cdot x_i + b - y_i \le \varepsilon + \zeta_i^* \\ \zeta_i \ge 0 \qquad i = 1, 2...n \\ \zeta_i^* \ge 0 \qquad i = 1, 2...n \end{cases}, \tag{4}$$

where C is penalty factor.

To solve Eq. (4), the Lagrange function is introduced to transform SVM regression formula as follow:

$$y' = \sum_{i=1}^{n} (\alpha_i - \alpha_i^*) K(x_i, x_j) + b \ , \tag{5}$$

where α_i and α_i* are lagrange multipliers, $K(x_i, x_j)$ is the radial basis function. $K(x_i, x_j)$ is shown as:

$$K(x_i, x_j) = \exp(-\frac{\|x - x_i\|}{\delta^2}) \ , \tag{6}$$

where δ is the bandwidth of the kernel function.

3.2 Back Propagation Neural Network (BPNN)

BPNN is developed from the forward perceptron network, and is a very mature and reliable neural network [19]. In the 1980s, Error Back Propagation Training is developed and is applied in forward neural network, and thus BPNN is generated.

We use a BPNN with three layers as example. As shown in Fig. 4, a normal BPNN has at least one input layer, one hidden layer and one output layer. Assume the input layer has n units, the hidden layer has m units and the units in the output layer is l. For the input data $\{x_1, x_2, ..., x_n\}$, the data will be processed as Eq. (7) to obtain the value h in hidden layer.

$$h_m = f(\sum_{i=1}^{n} w_{ij} x_i - a_j), j = 1, 2, ..., m \ , \tag{7}$$

where w_{ij} is the weight coefficient, a_j is the bias.

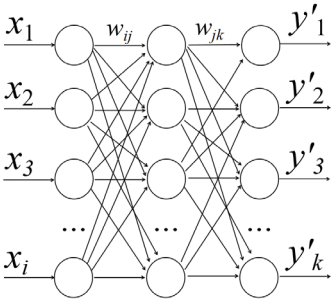

Fig. 4. The architecture of BPNN

Then the value $\{h_1, h_2, ..., h_l\}$ will be processed as Eq. (8) to obtain the value y' in hidden layer.

$$y'_k = f(\sum_{j=1}^{m} w_{jk} h_j - b_k), k = 1, 2, ..., l \ . \tag{8}$$

y' is the regression and the error between y' and y will be calculated for backward propagation to optimize the parameters of neural network. Backward propagation is a quite mature algorithm, so this paper will not introduce the backward propagation algorithm.

4 LSTM Network

In addition to the traditional machine learning algorithm, depth neural network has the stronger fitting performance. Recurrent neural network (RNN) is the network which is suitable for time series modeling. RNN is mainly used for processing sequence data. Its feature is that the output of the neuron at a certain time can be input to the neuron again as input data [20]. As shown in Fig. 5, this kind of network's architecture is very suitable for time series data and can maintain the dependency relationship.

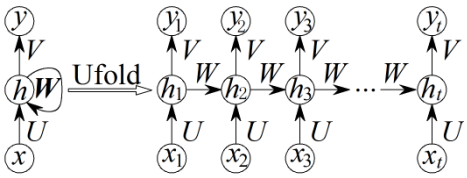

Fig. 5. The architecture of RNN

From Fig. 5, we can see the sequence $\{x_1, x_2, x_3, ..., x_t\}$ is inputted into hidden layer one by one. Different from the traditional feed forward neural network, in the hidden layer cells, there has information passing between hidden layers. So, RNN can express the time-dependent characteristics.

However, the performance of RNN is still insufficient, which can not solve the problem of gradient explosion and gradient vanishing. So, on the basis of RNN, researchers have developed some types neural network with gate structures and thus obtaining the stronger nonlinear performance. LSTM network is the most classic one.

4.1 Long-Short Term Memory Network (LSTM)

LSTM network was first proposed in 1997 [20]. Its main purpose is to solve the long-term dependence problem in recurrent neural networks. The difference between LSTM and RNN is in the composition of the hidden cell, and one LSTM cell is shown in Fig. 6.

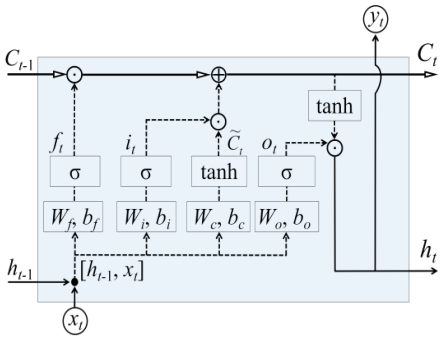

Fig. 6. LSTM cell in the hidden layer of the network

From Fig. 6, LSTM network adds three gates in hidden cell to control the processing of the information. These gates are actually composed of Sigmoid function and Tanh function. The retention degree of Sigmoid function is between 0 and 1 and the retention degree of Tanh function is -1 to 1, so the scope of the information can be controlled.

If using formulas to explain the gate structure in LSTM, the relevant formulas are shown as follows.

The activation functions are Sigmoid function and Tanh function, which are commonly used in neural network, as shown in Eq. (9) and Eq. (10) respectively.

$$\sigma(z) = \frac{1}{1+e^{-z}}\ , \tag{9}$$

where z is the input of the neurons.

$$\tanh(z) = \frac{e^{z} - e^{-z}}{e^{z} + e^{-z}} \ . \tag{10}$$

For the input data, LSTM network cell performs calculation as the following equations:

$$\tilde{C}_t = \tanh(W_c[h_{t-1}, x_t] + b_c) \ , \tag{11}$$

$$f_t = \sigma(W_f[h_{t-1}, x_t] + b_f) \ , \tag{12}$$

$$i_t = \sigma(W_i[h_{t-1}, x_t] + b_i) \ , \tag{13}$$

$$o_t = \sigma(W_o[h_{t\ 1}, x_t] + b_o) \ , \tag{14}$$

$$C_t = i_t * \tilde{C}_t + f_t * C_{t-1} \ , \tag{15}$$

$$y_t = h_t = o_t * \tanh C_t \ , \tag{16}$$

where W_c, W_f, W_i, W_o are weight coefficients; b_c, b_f, b_i, b_o are biases; $\tilde{C}_t$ and C_t represent the information of the internal state; f_t, i_t, o_t, b_o are the information gates; y_t and h_t represents the output information.

4.2 Nested Long-Short Term Memory Network (NLSTM)

Although LSTM has the strong nonlinear fitting performance, it may still face the problem of gradient disappearance in some complex tasks and long-time tasks. To solve the defects of LSTM, the Nested Long-Short Term Memory network was developed to obtain the stronger nonlinear fitting performance [21].

As shown in Fig. 7, the NLSTM cell is developed on the basis of LSTM. One NLSTM cell can be understood as being increased the depth in the cell, that is, NLSTM has a deeper architecture than LSTM. The data flow of NLSTM can be expressed by the following equations:

$$f_t = \sigma(W_f[h_{t-1}, x_t] + b_f) , \tag{17}$$

$$i_t = \sigma(W_i[h_{t-1}, x_t] + b_i) , \tag{18}$$

$$o_t = \sigma(W_o[h_{t-\ }, x_t] + b_o) , \tag{19}$$

$$\tilde{x}_t = i_t * \sigma(W_c[h_{t-1}, x_t] + b_c) , \tag{20}$$

$$\tilde{h}_{t-1} = f_t * C_{t-1} , \tag{21}$$

$$\tilde{f}_t = \sigma(\tilde{W}_f[\tilde{h}_{t-1}, \tilde{x}_t] + \hat{b}_f) , \tag{22}$$

$$\tilde{i}_t = \sigma(\tilde{W}_i[\tilde{h}_{t-1}, \tilde{x}_t] + \tilde{b}_i) , \tag{23}$$

$$\tilde{o}_t = \sigma(\tilde{W}_o[\tilde{h}_{t-1}, \tilde{x}_t] + \hat{b}_o) , \tag{24}$$

$$\tilde{C}_t = \tilde{f}_t * \tilde{C}_{t-1} + \tilde{i}_t * \sigma(\tilde{W}_c[\tilde{h}_{t-1}, \tilde{x}_t] + \tilde{b}_c) , \tag{25}$$

$$C_t = \tilde{o}_t * \sigma(\tilde{C}_t), \tag{26}$$

$$y_t = h_t = o_t * C_t. \tag{27}$$

where $\tilde{W}_f$, $\tilde{W}_i$, $\tilde{W}_o$, $\tilde{W}_c$ are weight coefficients; $\tilde{b}_f$, $\tilde{b}_i$, $\tilde{b}_o$, $\tilde{b}_o$ are biases; $\tilde{x}_t$ and $\tilde{h}_t$ represent the internal information.

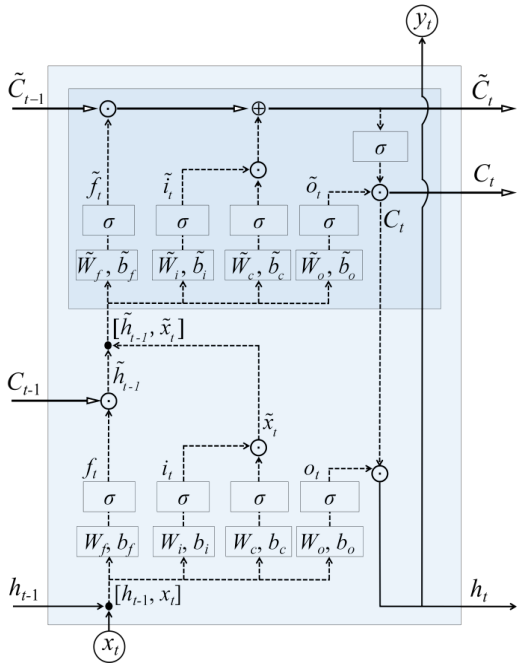

Fig. 7. NLSTM cell in the hidden layer of the network

The above fitting tools will be tested for selecting the best modeling scheme.

5 Data Flow and Evaluation Indicator

5.1 Learning Strategy and Data Flow of Model

In this paper, the supervised learning mode is used to establish the corresponding relationship between temperature data and deflection data. The data is divided into the training set and the test set. The training set is used to train the network, and the back-propagation is used to complete the gradient descent and update the network parameters. Finally, the neural network with excellent fitting performance is obtained. In this paper, the first 75% of the total data is taken as the training set, and the last 25% as the test set.

As shown in Fig. 8, the training process is common for different modeling tools. After the data is divided into training/test sets, the data is normalized and is brought into the network. The output data *y*' is compared with the real value for calculating loss, and the mean square error (*MSE*) is used as the loss value for back propagation to optimize the network. So far, an iteration is completed. The architecture of all networks used in this paper has one input layer, one hidden layer, one full connection layer and one output layer.

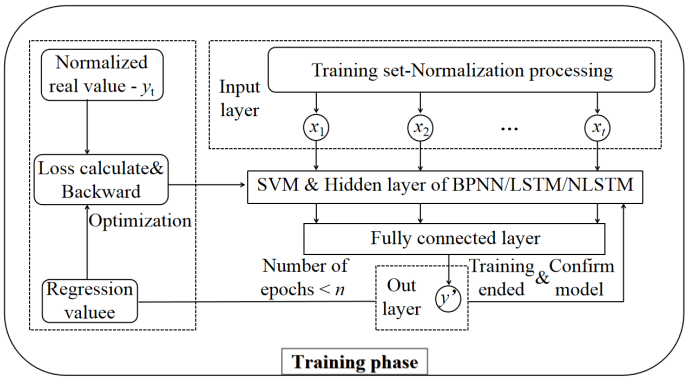

Fig. 8. Training process of machine learning algorithms

For the cable bridge, the response data of and the temperature data during the previous five hours data are most strongly correlated [8]. Therefore, the input model data is 5 hour temperature data (30 data points). The learning mechanism established in this paper is to fit the deflection data of the next moment with the temperature information of the past period, and its supervised learning strategy is shown in Fig. 9. The temperature data T in the previous 30 moments corresponds to the deflection data D of the next moment, and so on to complete the input and output project.

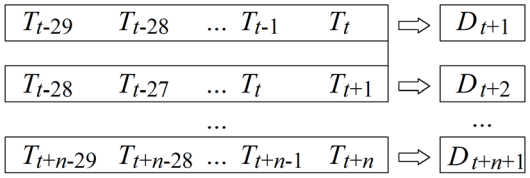

Fig. 9. Supervised learning mechanism

5.2 Evaluation Indicators

Evaluating the performances of different models to seek the fitting tool with the optimal performance, some indicators is needed to be developed to evaluate the output results of different models. For the regression model, the first thing we pay attention to is its output accuracy, so we use mean squared error (*MSE*) to evaluate its accuracy, and *MSE* can be calculated as follow:

$$MSE = \frac{\sum_{n=1}^{N} (D'_n - \overline{D})^2}{N}, \tag{28}$$

where N is the number of data points in the dataset, D'_n is the nth regression value, $\overline{D}$ is the mean of the true data.

In addition to well precision, we want to spend less time in training the neural network, that is, we want to build the model more efficiently. To evaluate the efficiency of the model, an index to comprehensively evaluate efficiency is established as η. This index is the product of model training time t and model error *MSE*, η, as shown in Eq. (29):

$$\eta = t \times MSE\ . \tag{29}$$

Next, we will test and evaluate the models established by different methods to select the best tool for regressing the temperature deflection of cable-stayed bridges.

6 Test and Discussion

This paper will test the trained SVM, BPNN, LSTM and NLSTM, and compare the machine learning results with the result of traditional regression analysis.

6.1 Calculation Results of Different Methods

According to the regression model established by D and T, the fitting formula was $D = -1.66T + 497.857$, and the goodness of fit is 0.684. Take the test set into the regression equation, and the comparison between the real value and the regression value is shown in Fig. 10. The *MSE* of the linear regression results is 74.14 mm^2. Obviously, the precision of the linear regression method is useless. Continue to test the models obtained by machine learning methods.

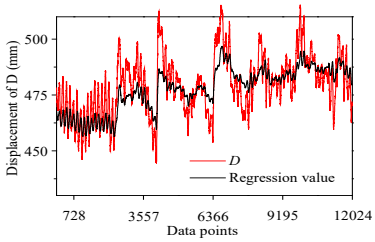

Fig. 10. Linear regression result

The normalized loss curve during training phase of the SVM model is shown in Fig. 11(a). After training with 100 epochs, the model is convergent. We take the test set into the trained SVM, the output result is shown in Fig. 11(b). Only by observation, the performance of SVM is significantly improved compared with the linear regression model, but the SVM result is still unsatisfactory. The *MSE* of the SVM results is 55.22 mm^2.

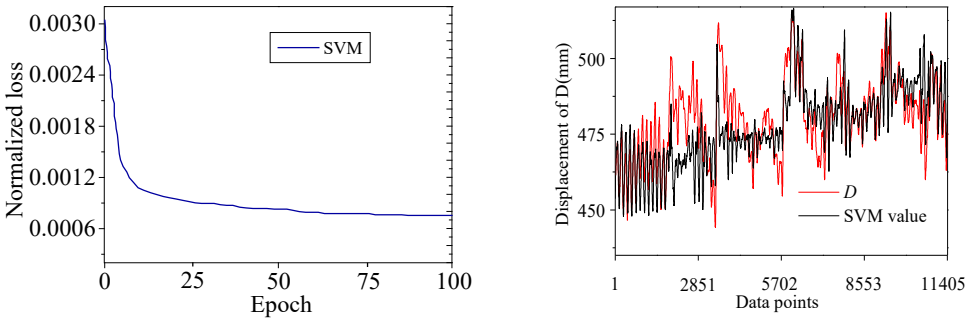

(a) Loss curve of the training of SVM model (b) Regression result of SVM model

Fig. 11. SVM regression result

The normalized loss curve during training phase of the BPNN model is shown in Fig. 12(a). After training with 100 epochs, the model is convergent. The result of the trained BPNN is shown in Fig. 12(b). Undoubtedly, the effect of artificial neural network is better than SVM model. The *MSE* of the BPNN results is 46.53 mm^2.

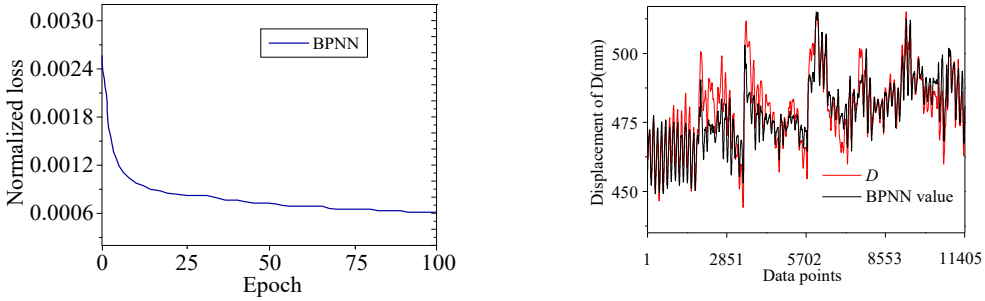

(a) Loss curve of the training of BPNN model (b) Regression result of BPNN model

Fig. 12. BPNN regression result

Next, the result of LSTM is shown in Fig. 13(a) and Fig. 13(b). The result of LSTM is better than that of BPNN, showing the advantage of deep neural network. The *MSE* of the LSTM results is 31.83 mm^2.

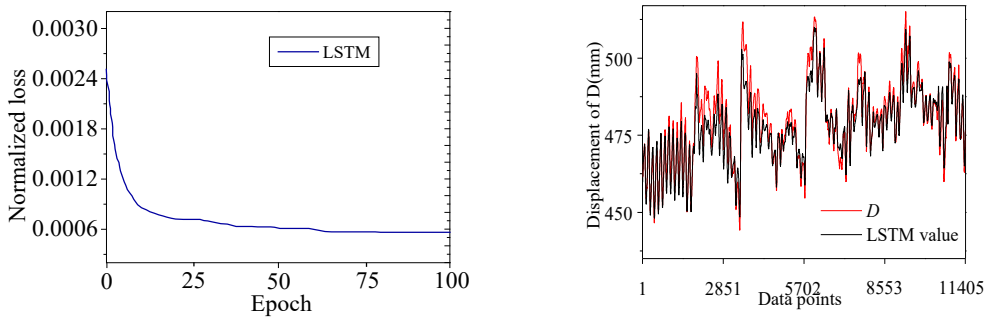

(a) Loss curve of the training of LSTM model (b) Regression result of LSTM model

Fig. 13. LSTM regression result

The result of NLSTM is shown in Fig. 14. The result of NLSTM is better than LSTM and is the best in different methods, showing the progressiveness of improved deep neural network. The *MSE* of the NLSTM results is 20.83 mm^2.

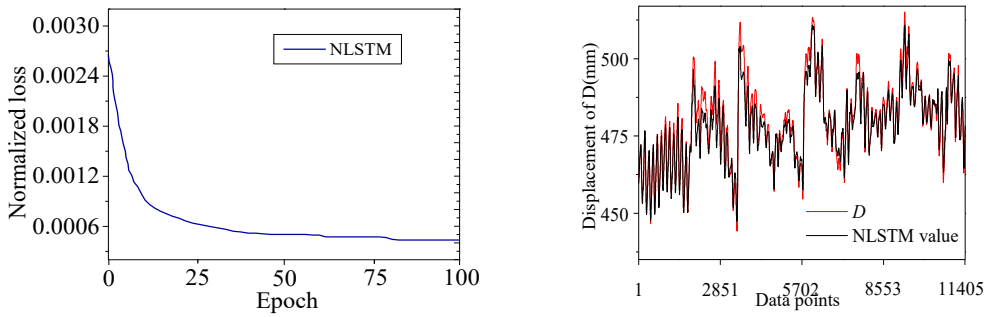

(a) Loss curve of the training of NLSTM model (b) Regression result of NLSTM model

Fig. 14. NLSTM regression result

6.2 Discussion on Optimal Model

As shown in Fig. 15, NLSTM is undoubtedly the best fitting tool only by precision. However, the evaluation of a model requires not only the precision, but also the training and the comprehensive efficiency of the model.

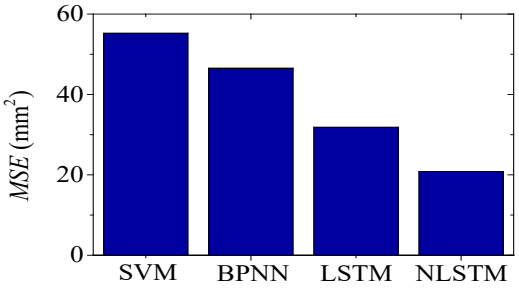

Fig. 15. Mean squared error of different fitting methods

The training of SVM is 112 s; the training of BPNN is 225 s; the training of LSTM is 322 s; the training of NLSTM is 823 s. The comprehensive efficiency of the model should be expressed by η. The smaller the η, the higher the efficiency. The η of different model is shown as Fig. 16 as below.

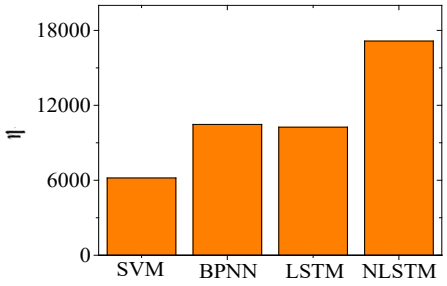

Fig. 16. Comprehensive efficiency (η) of different fitting methods

As shown in Fig. 16, the comprehensive efficiency of SVM is best, however the precision of SVM is not enough. In the other three models, LSTM not only has the best comprehensive efficiency which is massively smaller than that of NLSTM, but also at the same time, it is not much worse than NLSTM in precision. So LSTM is considered as the optimal fitting tool for building the model of the deflection of the cable stayed bridge.

6.3 Abnormal State Recognition Based on Statistical Pattern

The value output by the LSTM model can be used as the control value of the normal state, by the statistical pattern of t-test, the abnormal deflection can be recognized. We set the abnormal deviations from 0.5% to 15%. The test results is H1 and H0. H1 means the abnormal can be recognized and H0 means the abnormal can't be recognized. The result of t-test can be seen in Table 1.

Table 1. The results of t-test by LSTM model

Deviation (%)	t-test
15	H1
10	H1
8	H1
6	H1
4	H0
2	H0
1	H0
0.5	H0
0.25	H0

As shown in Table 1, 6% is the minimal abnormal deviation which can be recognized by the LSTM control value and the statistical pattern of t-test. To sum up, the temperature-induced deflection modeling of cable-stayed bridge is a highly nonlinear project. By using the machine learning LSTM network, the output precision can

be improved a lot than the traditional methods. The LSTM model is the optimal fitting tool considering both precision and modeling efficiency. Recognizing 6% abnormal deflection is positive for operation and maintenance of the cable-stayed bridge.

7 Conclusions

(1) The precision of the traditional linear regression analysis can not meet the requirements of bridge monitoring. With the progress of computer technology, machine learning tools should be explored whether can be used to establish the high-precision deflection model of cable-stayed bridges. Considering both the precision and modeling efficiency, LSTM is the optimal tool which can reach the precision of mean square error as 31.83 mm^2.

(2) Use the regression value output by LSTM as the control value combining with the statistical pattern of t-test, the 6% abnormal deflection can be recognized. This recognizing value is really small and thus has the positive value for operation and maintenance of the cable-stayed bridge.

8 Acknowledgments

This research was supported by the National Key Research and Development Program (Grant No. 2019YFB1600702), Shenzhen Technology Research Project (Grant No. CJGJZD20210408092601005) and National Natural Science Foundation of China (Grants 51978154, 52008099, and 51608258).

References

[1] Q.-W. Zhang, Conception of Long-span Bridge Health Monitoring and Monitoring System Design, Journal of Tongji University: Natural Science Edition 29(1)(2001) 65-69.
[2] B. Hunt, N. Cooke, Thermal calculations for bridge design, Journal of the Structural Division 101(9)(1975) 1763-1781.
[3] W. Zuk, Thermal and shrinkage stresses in composite bridges, Journal of the American Concrete Institute 58(3)(1961) 327-340.
[4] M.J.N. Priestley, Design thermal gradients for concrete bridges, New Zealand Engineering 31(9)(1976) 213-219.
[5] M.J.N. Priestley, Design of concrete bridges for temperature gradients, Journal of the American Concrete Institute 75(5) (1978) 209-217.
[6] P.C. Hoffman, R.M. McClure, H.H. West, Temperature study of an experimental segmental concrete bridge, Journal of the Prestressed Concrete Institute 28(2)(1983) 78-97.
[7] H.-C. Fu, S.F. Ng, M.S. Cheung, Thermal behavior of composite bridges, Journal of Structural Engineering 116(12) (1990) 3302-3323.
[8] X. Liao, Y. Wang, L. Feng, Y.J. Shi, Investigation on fatigue crack resistance of q370qE bridge steel at a low ambient temperature, Construction and Building Materials 236(2020) 117566.
[9] S. Li, H. Lv, Y. Kuang, N. Deng, C. Sun, X. Zhao, Force-monitoring ring based on white-light interferometry for bridge cable force monitoring and its temperature compensation, Advances in Structural Engineering 22(6)(2019) 1444-1452.
[10]X.-F Liu, Computation of Temperature Stresses For Prestressed Concrete Box Girders, China Civil Engineering Journal (1)(1986) 44-54.
[11]C. Hao, R.X. Ding, S.Q. Liu, Numerical simulation of temperature field distribution of steel bridge, World bridges (3) (2002) 59-62.
[12]J. Lee, K.J. Loh, H.S. Choi, H.Y. An, Effect of Structural Change on Temperature Behavior of a Long-Span Suspension Bridge Pylon, International journal of steel structures 19(6)(2019) 2073-2089.
[13]Y.-L. Ding, G.X. Wang, G.-D. Zhou, A.-Q. Li, Life-cycle simulation method of temperature field of steel box girder for Runyang cable-stayed bridge based on field monitoring data, China Civil Engineering Journal 5(2013) 129-136.
[14]L. Liu, G. Meng, A Two-Step Approach to Identify Damage Location Based on Curvature Modal Parameters and Support Vector Machine, Engineering mechanics 23(S1)(2006) 35-39.
[15]T.H.T. Chan, Y.Q. Ni, J.M. Ko, Neural network novelty filtering for anomaly detection of Tsing Ma Bridge cables, Structural health monitoring (2000) 430-439.
[16]H. Liu, Y.-L. Ding, H.-W. Zhao, M.-Y. Wang, F.-F. Geng, Deep learning-based recovery method for missing structural temperature data using LSTM network, Structural Monitoring and Maintenance 7(2)(2020) 109-124.
[17]G. Hinton, L. Deng, D. Yu, G.E. Dahl, A. Mohamed, N. Jaitly, A. Senior, V. Vanhoucke, P. Nguyen, T.N. Sainath, B. Kingsbury, Deep Neural Networks for Acoustic Modeling in Speech Recognition: The Shared Views of Four Research Groups, IEEE Signal Processing Magazine 29(6)(2012) 82-97.
[18]V. Cherkassky, Y. Ma, Practical selection of SVM parameters and noise estimation for SVM regression, Neural Networks 17(1)(2004) 113-126.
[19]K. Cherifi, An overview on recent machine learning techniques for Port Hamiltonian systems, Physica D: Nonlinear

Phenomena 411(2020) 132620.
[20]S. Hochreiter, J. Schmidhuber, Long short-term memory, Neural computation 9(8)(1997) 1735-1780.
[21]Z. Yu, G. Liu, Q. Liu, J. Deng, Spatio-Temporal Convolutional Features with Nested LSTM for Facial Expression Recognition, Neurocomputing 317(2018) 50-57.